

Hydrologic Loading Model Displacements from the National and Global Data Assimilation Systems (NLDAS and GLDAS)

February 13, 2017

Authors

Christine M. Puskas¹

Charles M. Meertens¹

David Phillips¹

¹UNAVCO Geodetic Data Services Group

Hydrologic Surface Loading and Poroelastic Effects

Water in the Earth is stored in oceans, lakes, rivers, groundwater reservoirs, as well as in snowpack, soil, and vegetation. In continental interiors, groundwater and surface water predominate. The mass of water varies seasonally and is large enough to produce displacements of several mm in GPS time series (Herring et al., 2016). The water mass also varies geographically, depending on climate (Fovell and Fovell, 1993) and local geology (Miller, 1994). These mass variations are part of the water cycle.

Ground deformation changes in water storage can be divided into elastic and poroelastic components. Elastic deformation occurs from water mass changes at the Earth's surface from water bodies (lakes, rivers, etc.) and from snowpack, soil, and vegetation. When there is more precipitation during winter or the rainy season, the water goes into these storage media (Figure 1). The weight of the extra water depresses the ground surface, which deforms elastically in response to the load. In the summer or dry season when evaporation and runoff exceeds precipitation, surface water mass decreases and the earth rebounds, producing uplift (Wahr et al., 2013; van Dam et al., 2001; Meertens et al., 2011).

Poroelastic deformation is produced by changes in groundwater storage (Figure 2).

Groundwater is stored in aquifers, or formations of porous and permeable sediments and rocks, and aquitards, or formations of low-permeability silts and clay (Miller, 1994). When water is withdrawn from an aquifer or aquitard, pore spaces that were previously supported by water pressure are compacted and overlying ground surface subsides (Galloway et al., 1999). When aquifers are recharged from precipitation or seasonal streamflow, pores open again and the ground surface rises. In aquitards, the compaction is permanent and the resulting subsidence is permanent. Groundwater pumping drives poroelastic deformation in agricultural regions (Poland et al., 1975; Argus et al., 2014; Rodell and Famiglietti, 2002; Rodell et al., 2007; Wahr et al., 1998).

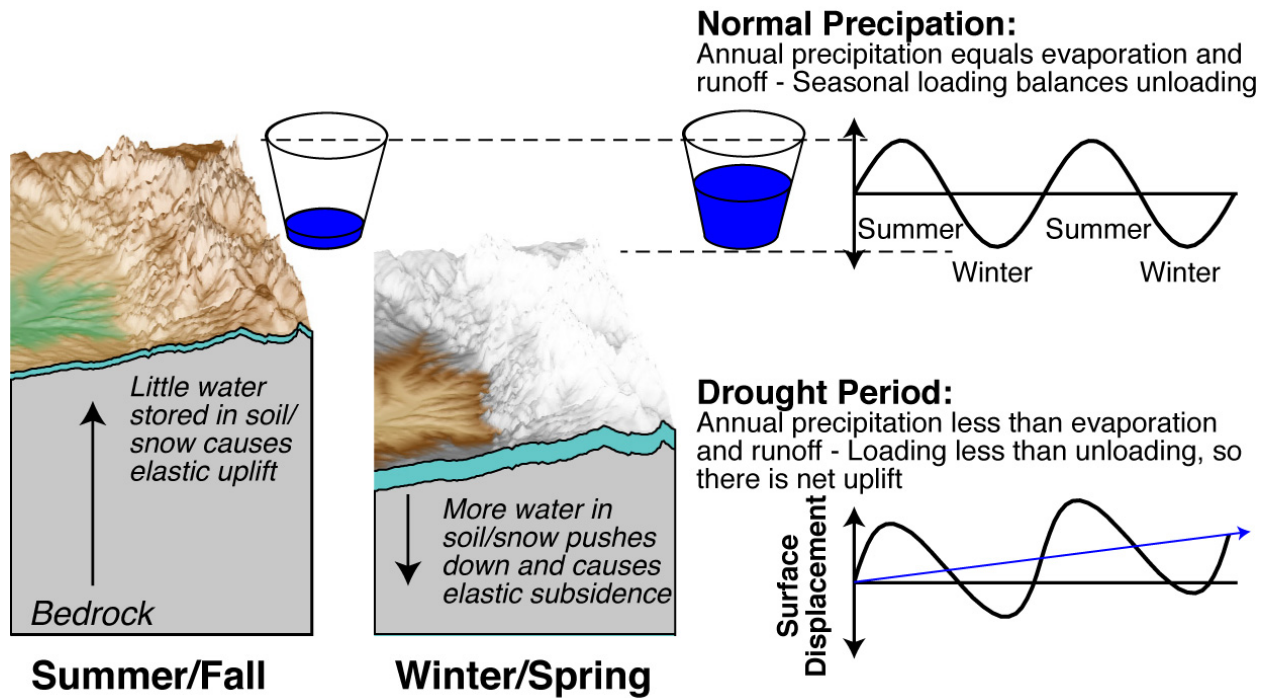


Figure 1. Schematic of hydrologic surface water loading (represented by cups) and resulting time series of vertical motion. During normal periods the annual precipitation rate keeps up with evaporation and runoff. During period of drought the water accumulation does not keep up and there is a longer period uplift. The example shown is for mountains in the northern hemisphere such as the Sierra Nevada mountains of California. The mountains are that the highest point in the late summer early fall when the water mass is at a minimum. They are at the lowest point in the seasonal cycle in late winter early spring when the snow accumulation is a maximum.

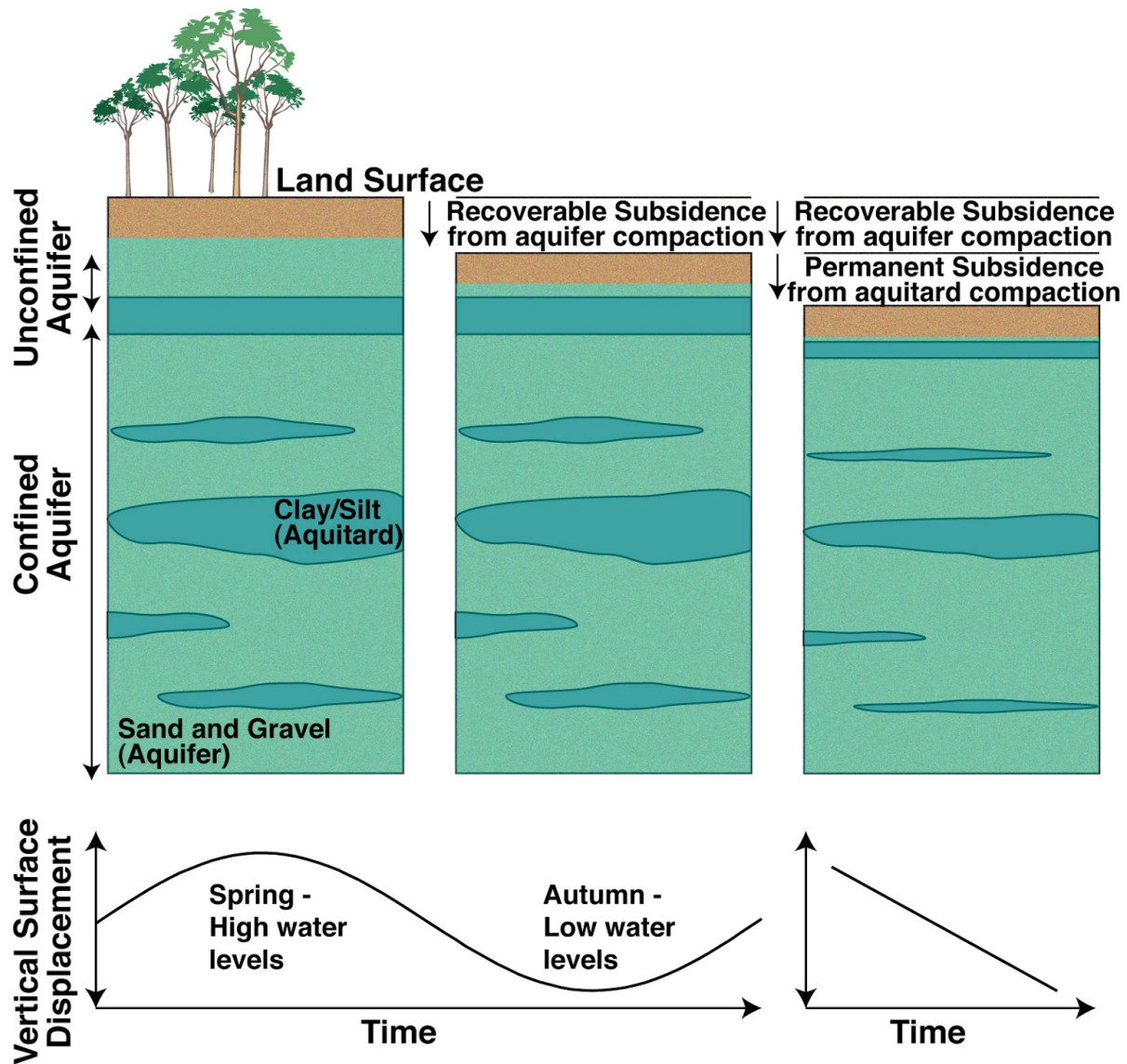


Figure 2. The mechanism for ground motion due to groundwater level changes is poroelastic effect. As shown in this figure modified from Galloway et al. (1999), when the water level drops the water no longer supports the soil matrix and the pore spaces are compacted. The opposite occurs when the water level rises. The motion is primarily in the vertical, but can affect the horizontal when localized pumping rates exceed local recharge. If pumping rates are large enough, water will be lost from the aquitards interspersed in the aquifer. Water stored in aquitards is not recharged, and aquitard compaction results in permanent subsidence. In contrast to the surface loading cycle in mountains such as the Sierra Nevada range, groundwater variations and poroelastic response in adjacent valleys is out of phase. The land surface in valleys is a maximum after spring runoff from the mountains has recharged the aquifers and a minimum in the Autumn when the groundwater levels are depleted by subsurface flow, pumping, and evaporation.

Hydrologic Data Products

We present displacement models for stations in the Plate Boundary Observatory (PBO) (Figure 3) based on hydrologic surface loading from land surface models (LSM) produced by the Global Land Data Assimilation System (GLDAS) and the National Land Data Assimilation System (NLDAS) (Mitchell et al., 2004; Rodell et al., 2004; Xia et al., 2012). In 2017 an updated global model GLDAS 2.1 was released and that will be integrated into loading models in 2017. These products address part of the seasonal loading signals observed in the Plate Boundary Observatory time series (Herring et al., 2016). The hydrologic surface loads are based on the mass of water stored as soil moisture, snow, and in vegetation.

The input GLDAS and NLDAS LSMs used to model displacement are monthly files, and our modeling codes interpolate to produce daily north, east, and vertical displacement time series at GPS station locations. These model loading displacements are derived entirely from the surface hydrologic loads and are independent of the GPS measurements.

The GLDAS-derived models use the Noah (1°), VIC (1°), and MOS (1°) LSMs to obtain surface loads due to soil moisture, snow, and vegetation water content on a 1° global grid (Figure 4). 3-D elastic displacements are calculated at specified station coordinates within the grid using Green's functions (Farrell, 1972) and the algorithms of van Dam et al. (2001) and Wahr et al. (2013). Contributions from loads at all grid squares are summed at coordinates corresponding to GPS station locations. Displacements are calculated for all stations within grid squares for which there are data available. Stations on coasts and islands that do not fall within the LSM data grids do not have displacements calculated. In the global grid, oceanic grid squares are set to zero and masked out.

During beta testing, we generated models based on the Noah 0.25° grid. The 0.25° data products were discontinued by the Goddard Earth Sciences (GES) Data and Information Services Center (DISC) at the end of 2016, so we will have files available at the UNAVCO ftp site through the end of 2016, but there will be no updates. Users looking for a finer resolution are encouraged to try the NLDAS models, which will be available in 2017.

The GES DISC has begun producing updated GLDAS v2.1 products in summer 2016, in addition to the GLDAS v1 products that UNAVCO has been using as a basis for modeling. Displacement models based on GLDAS v2.1 will be added to UNAVCO's hydrologic data products in 2017.

The NLDAS-derived model at this time uses the Noah LSM to obtain surface loads due to soil moisture and snow on a 0.125° grid with data available for the conterminous US (Figure 5). As with the GLDAS models, displacements are calculated for station coordinates within the grid, and stations outside the NLDAS grid area are not used.

Data files are released in a comma-separated (csv) format, with a header describing the data fields (Table 1). Current hydrologic data products can be downloaded from the UNAVCO ftp

server at <ftp://data-out.unavco.org/pub/products/hydro/>. The data products can also be downloaded from the UNAVCO web services site (<https://www.unavco.org/data/web-services/documentation/documentation.html#!/gps/getHydrologicalByStationId>). UNAVCO updates the hydro loading products on a quarterly basis.

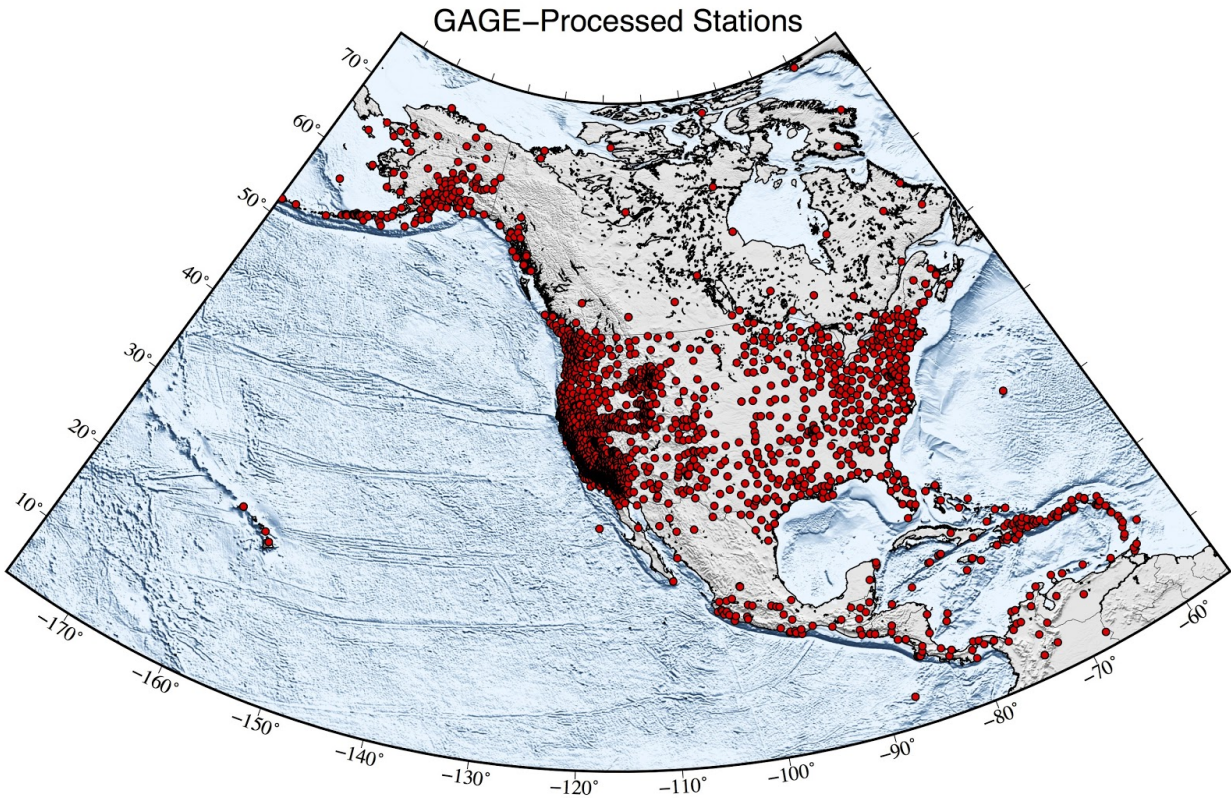


Figure 3. Map of stations in North America, Mexico, and the Caribbean region processed by the GAGE Analysis Centers. Hydrologic load models are computed for those stations that fall within the GLDAS and NLDAS model coverage areas.

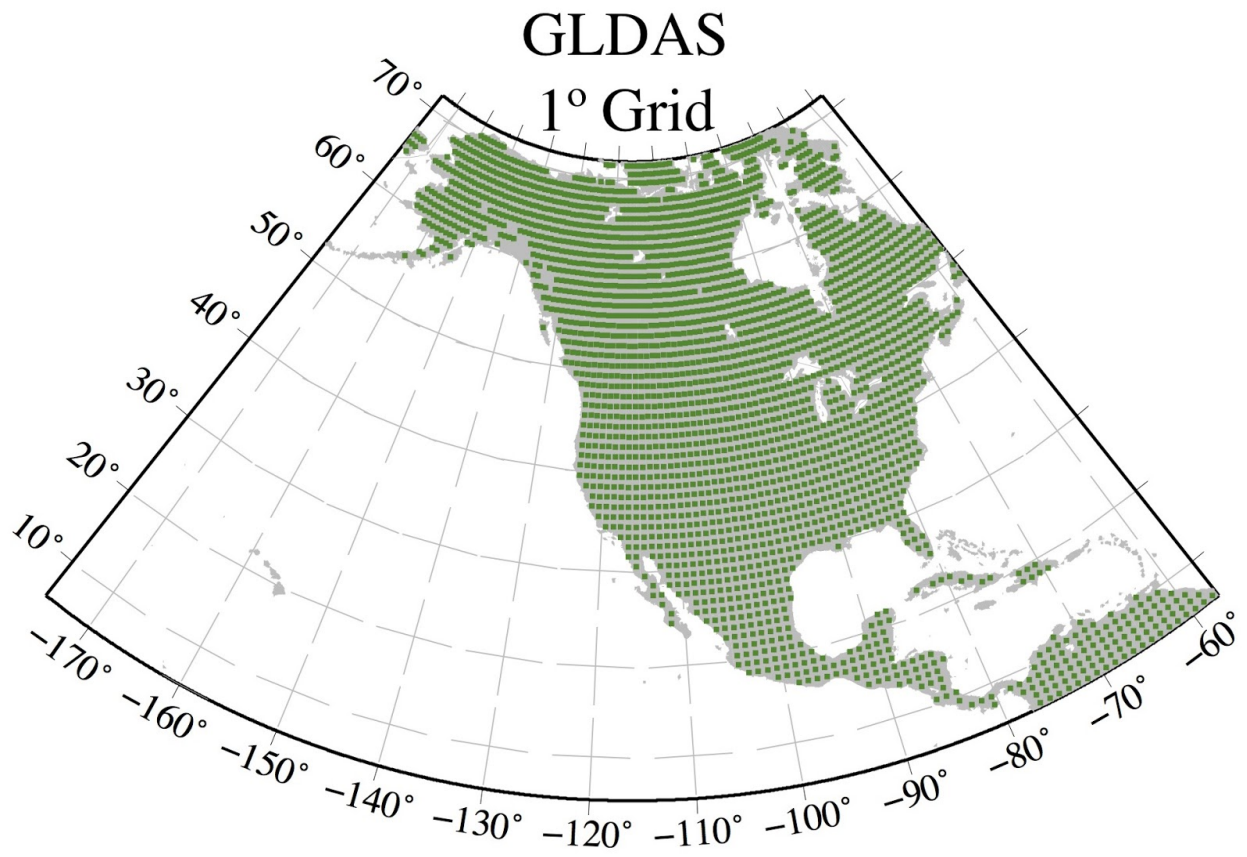


Figure 4. Distribution of grid squares in the GLDAS model for 1° grid. The GLDAS model uses a global grid, but only North America is shown.

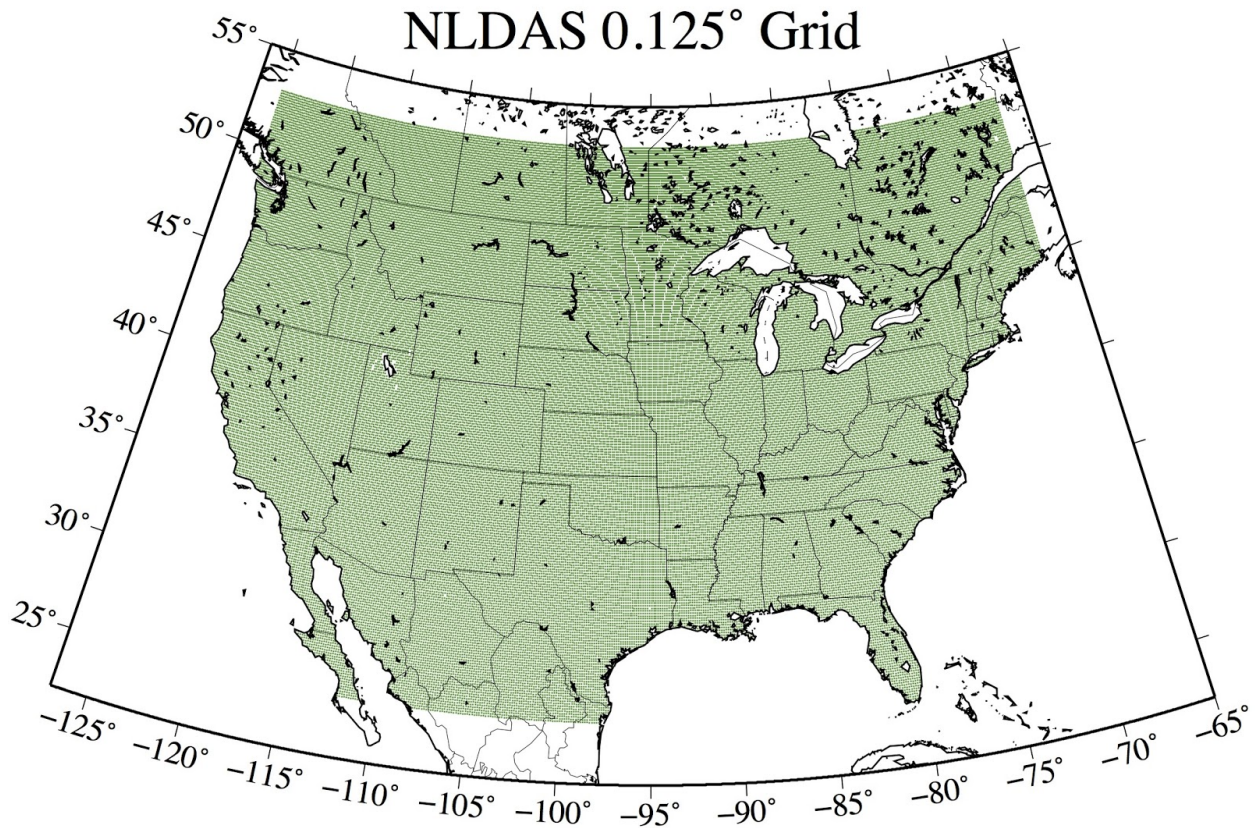


Figure 5. NLDAS grid map. The grid size is 0.125°, which correspond to squares of 8-13 km, depending on latitude.

Table 1. Hydrologic load model time series format. Columns are comma-delimited.

Column	Entry	Definition
1	Date	Date in year-month-day format
2	YYYY-DOY	Date in year-day of year format
3	MJD	Modified Julian Day
4	DispN	Modeled north displacement (mm)
5	DispE	Modeled east displacement (mm)
6	DispU	Modeled vertical displacement (mm)

Land Surface Models

The Global Land Data Assimilation System (GLDAS) and National Land Data Assimilation System (NLDAS) are projects to generate sets of environmental parameters by incorporating satellite and ground observations into land surface models using data assimilation techniques (Mitchell et al., 2004; Rodell et al., 2004; Xia et al., 2012).

GLDAS was developed through the collaboration between the National Aeronautics and Space Administration (NASA) Goddard Space Flight Center (GSFC) and the National Oceanic and Atmospheric Administration National Centers for Environmental Prediction (NOAA NCEP). GLDAS oversees multiple LSMs, developed and contributed by different groups. Current displacement models are based on GLDAS v1 (Rui, 2011), with plans to add models based on GLDAS v2.1 (Rui and Beaudoin, 2016) in 2017. Version 2.1 environmental data have been reprocessed with updated Princeton Forcing Data (Sheffield et al., 2006) and upgraded software, and contains fixes for biases found in version 1.

NLDAS was the result of collaboration between NCEP Environmental Modeling Center (EMC), NCEP Climate Prediction Center (CPC), GSFC, Princeton University, the National Weather Service Office of Hydrologic Development (NWS OHD), and the University of Washington, with support from NOAA's Modeling, Analysis, Predictions, and Projections (MAPP) Program. Like GLDAS, NLDAS oversees multiple LSMs, of which only the Noah model is currently used to produce station data products.

LSMs integrate surface environmental parameters for water, temperature, atmospheric pressure, radiation, fluxes, and other measures of the transfer of mass and energy at the Earth's surface. The GLDAS models have global coverage at resolutions ranging from 0.25° to 2.5° (Figure 4), while the NLDAS models are 0.125° for the conterminous US (Figure 5). Different LSMs use different methods for processing observations and modeling parameters. The primary differences relevant to UNAVCO's hydrologic modeling are due the number and thicknesses of the soil layers (Table 2)(Fang et al., 2009; Mitchell et al., 2004).

The GLDAS LSMs used to produce hydrologic displacement models are named NOAH (Noah) 1.0, MOS (Mosaic) 1.0, and VIC (Variable Infiltration Capacity) 1.0. Names may be abbreviated to NOAH10, MOS10, and VIC10, with the numbers referring to grid size in degrees. The NLDAS Noah LSM model was used to generate the NLDAS displacement model.

The Noah models were developed by the Global and Energy Water Cycle Experiment Continental-Scale International Project using a layered soil model and including a vegetation parameter for each grid square (Chen et al., 1996; Koren et al., 1999). NOAH is the model used in NCEP climate and weather models. The other LSMs are based on the same data and techniques, with variations in how soil moisture and canopy water storage are treated. The Mosaic model accounts for different vegetation types in each grid cell (Koster and Suarez, 1992; Koster and Suarez, 1996), although ultimately water stored in vegetation contributes little to surface loading in North America. The VIC model calculates the infiltration and drainage of water through the soil (Liang et al., 1994) and does not include vegetation at all.

Table 2. Number and depth distributions in GLDAS land surface models (Fang et al., 2009) and NLDAS land surface models (Mitchell et al., 2004).

Model Name	Number of Soil Layers	Depths of Layers (m)
GLDAS MOS (Mosaic) 1.0	3	1. 0-0.02 2. 0.02-1.50 3. 1.5-3.50
GLDAS NOAH 1.0	4	1. 0-0.1 2. 0.1-0.4 3. 0.4-1.0 4. 1.0-2.0
GLDAS VIC (Variable Infiltration Capacity) 1.0	3	1. 0-0.1 2. 0.1-1.6 3. 1.6-1.9
NLDAS NOAH	4	1. 0-0.1 2. 0.1-0.4 3. 0.4-1.0 4. 1.0-2.0

Hydrologic Load Models

Soil moisture, snow load, and total canopy water storage are part of the modeled parameters in the land surface model. They are derived from input forcing parameters that include precipitation, surface pressure, air temperature, specific humidity, long- and shortwave radiation, and wind (Rodell, 2004). The modeling of these parameters has evolved over time as studies have investigated the physics of diffusion and heat and moisture fluxes and refined the algorithms and parameterization of soil structure and land surface-atmospheric interactions (see Ek et al., 2003 and Chen et al., 1996 for a history of the evolution of the Noah LSM).

Soil moisture, snow load (also called snowpack and snow-water equivalent), and total canopy water storage are extracted from the LSMs for GLDAS and NLDAS. The input parameters and resulting modeled displacements are compared for selected GPS stations and GLDAS and NLDAS parameters (Figures 6-9). Two GPS sites were chosen for comparison: P571 in the Sierra Nevada foothills near Sequoia National Park, and P041 near Boulder, CO. Both stations are at the base of mountain ranges. The GLDAS grid squares that encompass them include part of the mountains and as a result have a higher snow load than the smaller NLDAS grid squares. Similarly, the NLDAS grid squares have higher soil moisture than the larger GLDAS squares. Because of the larger grid size, GLDAS values are more smoothed than the NLDAS models. Despite the smoothing in the GLDAS model, the resulting NLDAS and GLDAS displacement models are more similar to each other than to the detrended GPS time series. In the north component, the P571 displacement models track the GPS time series, while the P041

displacement models are clearly out of phase (Figure 9). This is likely due groundwater withdrawal near the site. Seasonal climatic cycles predict snow and higher soil content in the winter, causing subsidence, and drying in the summer, causing uplift. Groundwater pumping is higher in the summer for agricultural and consumer use but then is recharged over the winter, causing poroelastic subsidence and uplift (Meertens et al., 2011; Miller, 1994; Poland et al., 1975) rather than the elastic loading and rebound assumed by our models. Neither displacement model predicts significant motion in the east component, underestimating the GPS signal at both sites. Both sites underpredict the observed amplitudes in the vertical component, and are unable to model multi-year and short-term variations. We attribute the multiyear variations to climatic effects. Most notably a strong drought developed in California in 2011, and the seasonal amplitudes decreased as there was less water stored at the surface. At the same time, the loss of groundwater caused elastic rebound over a period of years, because P571 was located outside agricultural areas and so was not affected by poroelastic processes. The GLDAS and NLDAS models only account for surface loading, so when there are significant changes in water storage at depths, the model does not reflect these. The short-term variations (over periods of days) in the GPS time series are probably correlated with atmospheric loading. The GLDAS and NLDAS LSM files are produced on a monthly basis, so the resulting displacement models are smoothed in time. Both GPS stations experienced offsets in their time series because of equipment changes.

Water mass stored in vegetation is included in Figures 5 and 6, but is negligible ($< 1 \text{ kg/m}^2$).

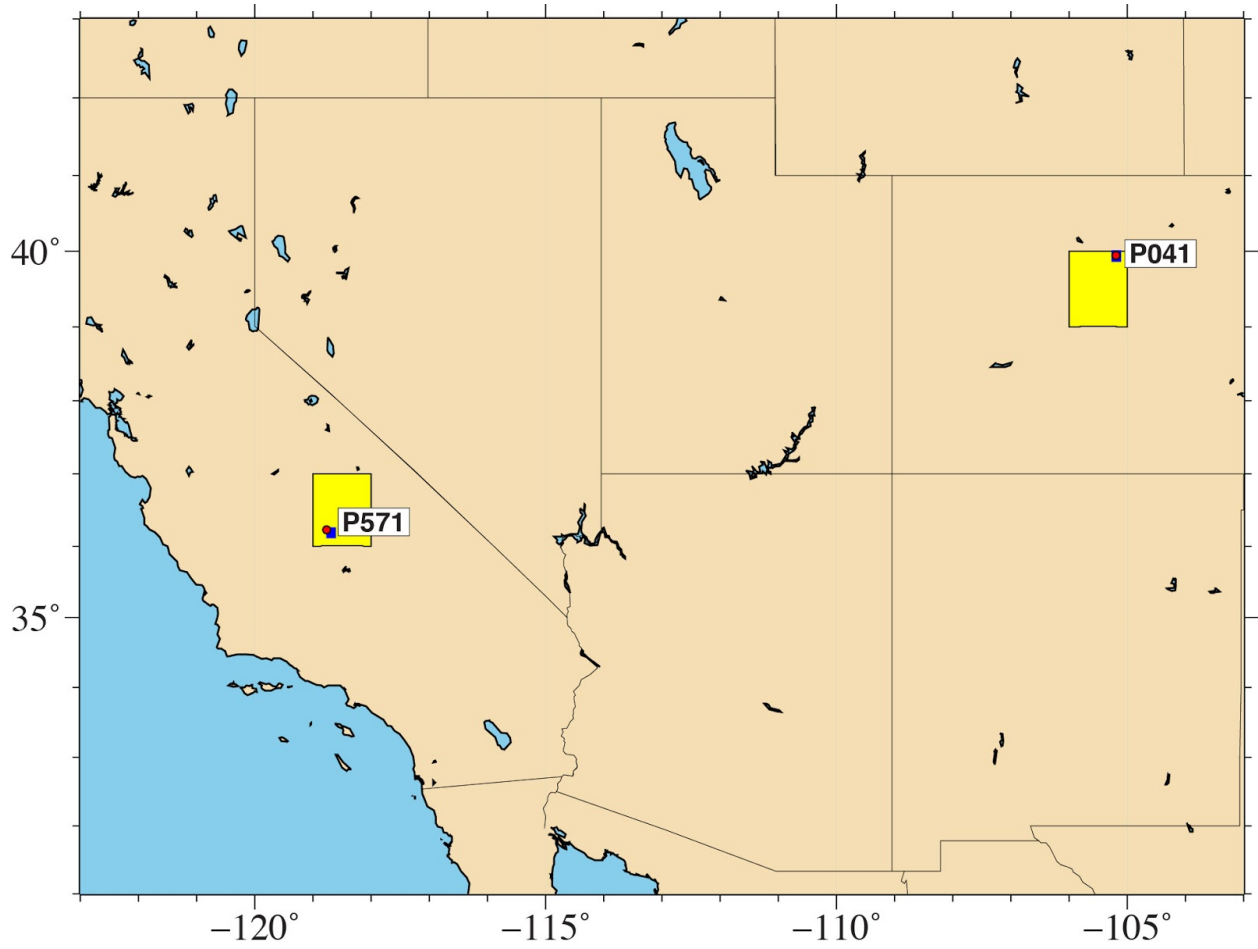


Figure 6. Index map of GLDAS grid square (yellow), NLDAS grid squares (blue), and GPS stations for which parameters and displacements were compared. P041 is located near Boulder, CO, and P571 is in the foothills of the Sierra Nevada.

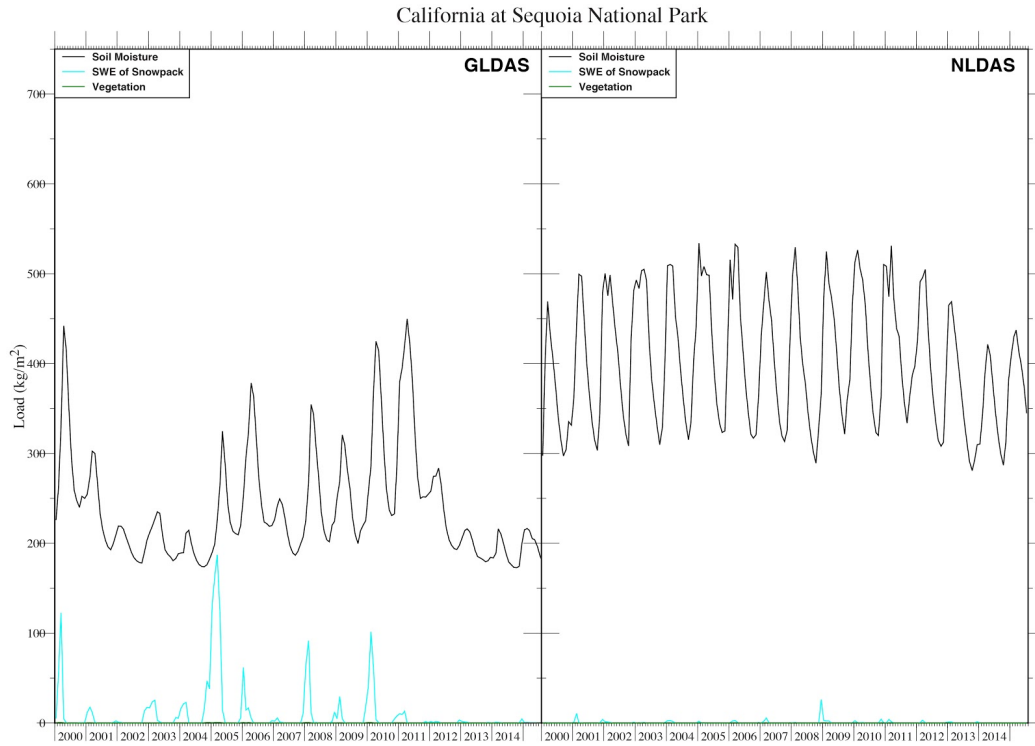


Figure 7. Comparison of GLDAS and NLDAS Noah LSM loading parameters near Sequoia National Park, in the foothills of the Sierra Nevada.

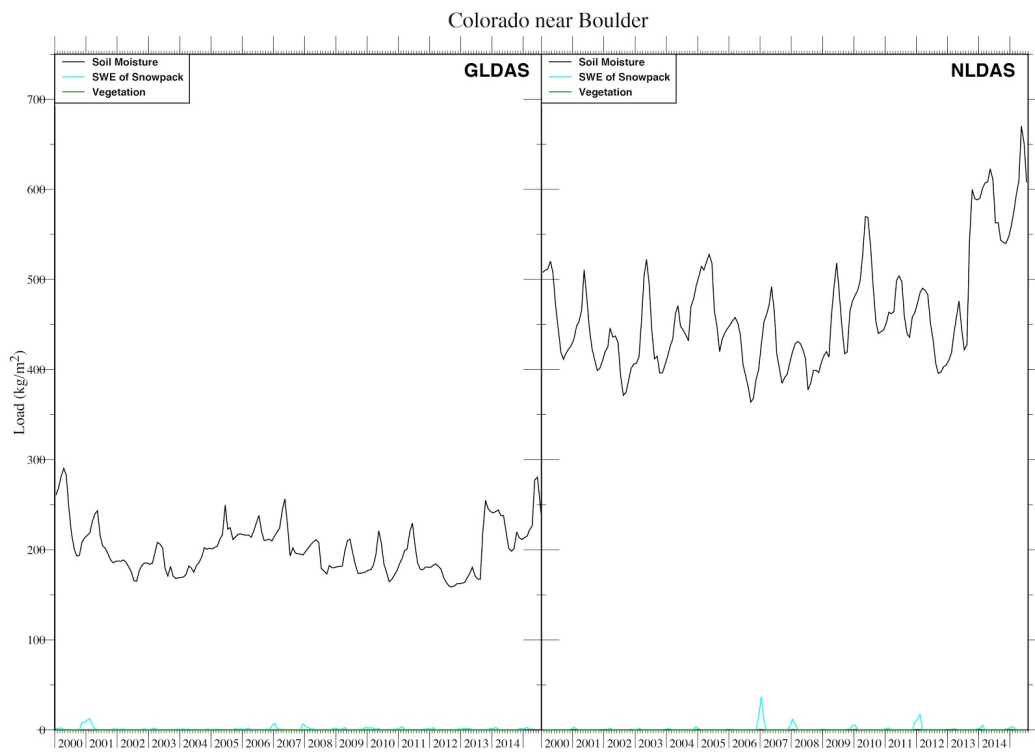
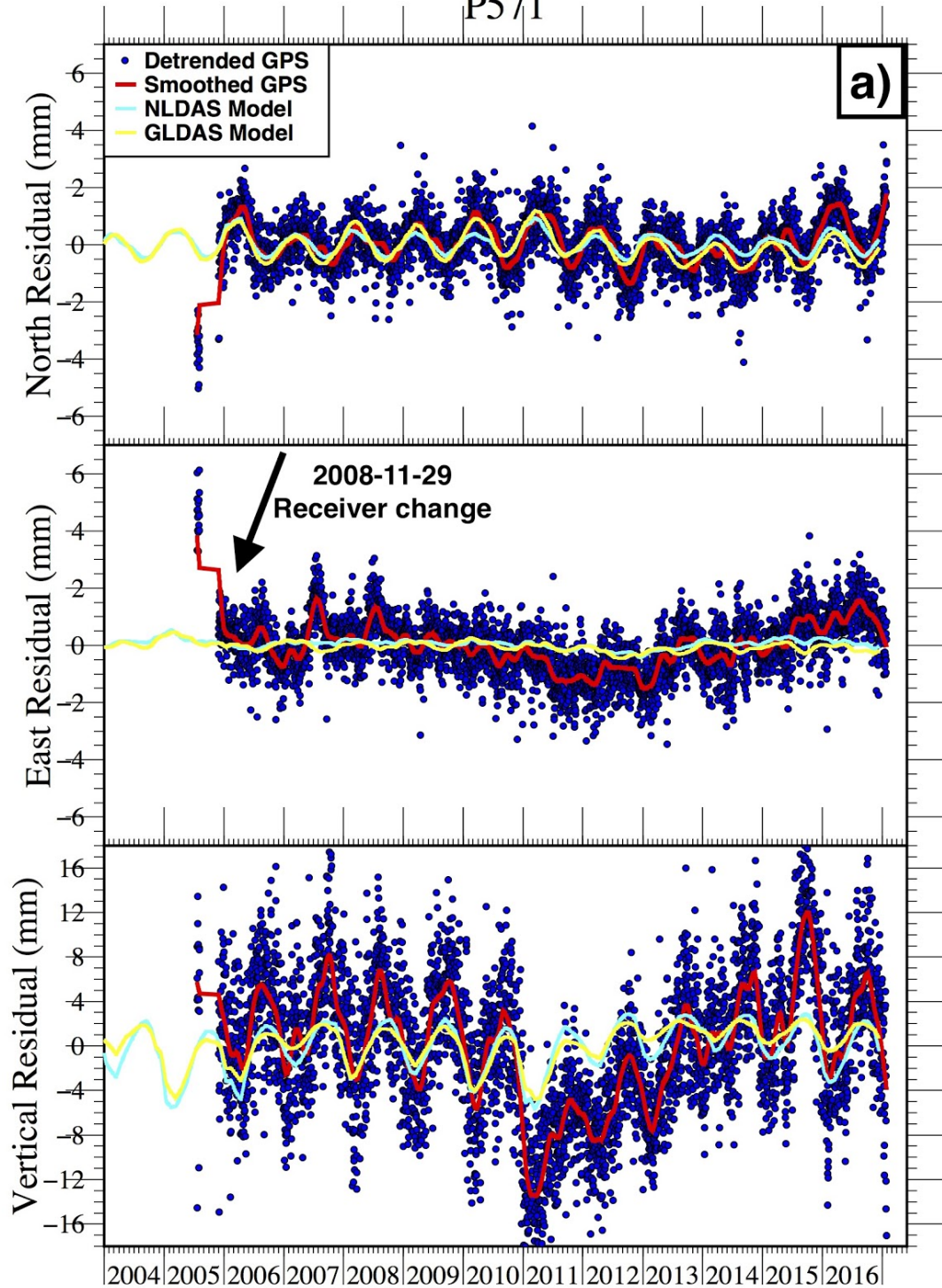


Figure 8. Comparison of GLDAS and NLDAS Noah LSM loading parameters near Boulder, Colorado.

P571



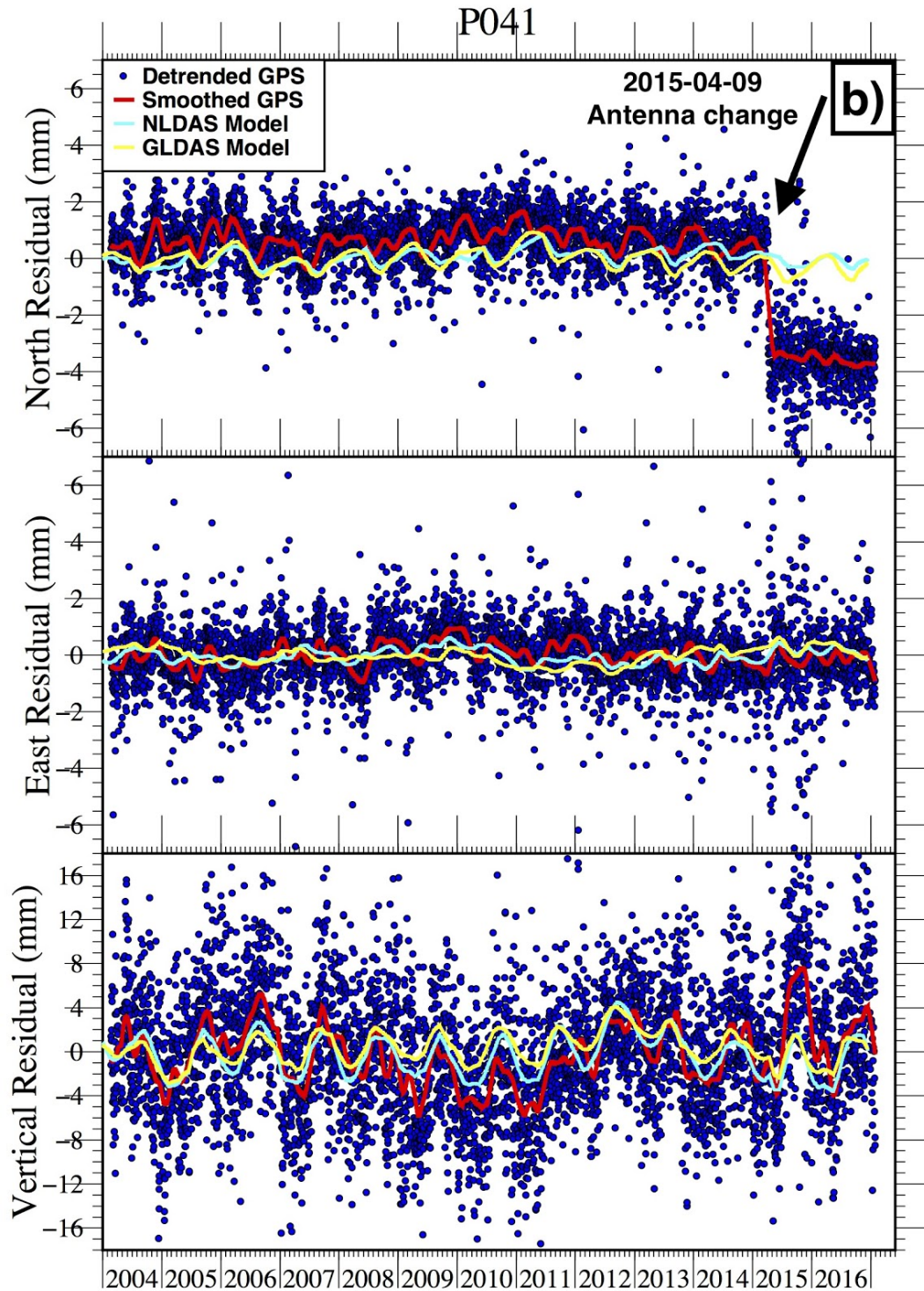


Figure 9. Comparison of detrended GPS time series, GLDAS displacement model, and NLDAS displacement model for a) P571 in the Sierra Nevada foothills and b) P041 near Boulder, CO. Offsets in the time series are due to a failed receiver in 2005 at P571, and an antenna replacement in 2015 at P041.

We include one more comparison to illustrate the difference between GLDAS and NLDAS loading. In Figure 10 we compare GLDAS and NLDAS soil moisture in February 2015. The NLDAS model predicts wetter soil for much of the US, and variations follow geographic features. For example, the eastern Snake River Plain in Idaho store more water in the soil than the surrounding mountains while the Nebraska Sand Hills are relatively dry. The GLDAS model predicts that much of the western US is dry ($<200 \text{ kg/m}^2$), except for the Pacific Northwest. In Figure 11, we compare snow water equivalent. Here the NLDAS model has high snow loads ($>200 \text{ kg/m}^2$) in the mountains while GLDAS has low snow loads ($<50 \text{ kg/m}^2$) everywhere. Note that because of the larger grid size, GLDAS can produce larger displacements with smaller loads. That is, for the same load distributed uniformly in a 1° grid and a 0.125° grid, the total mass in the 1° grid is larger, resulting in greater displacement.

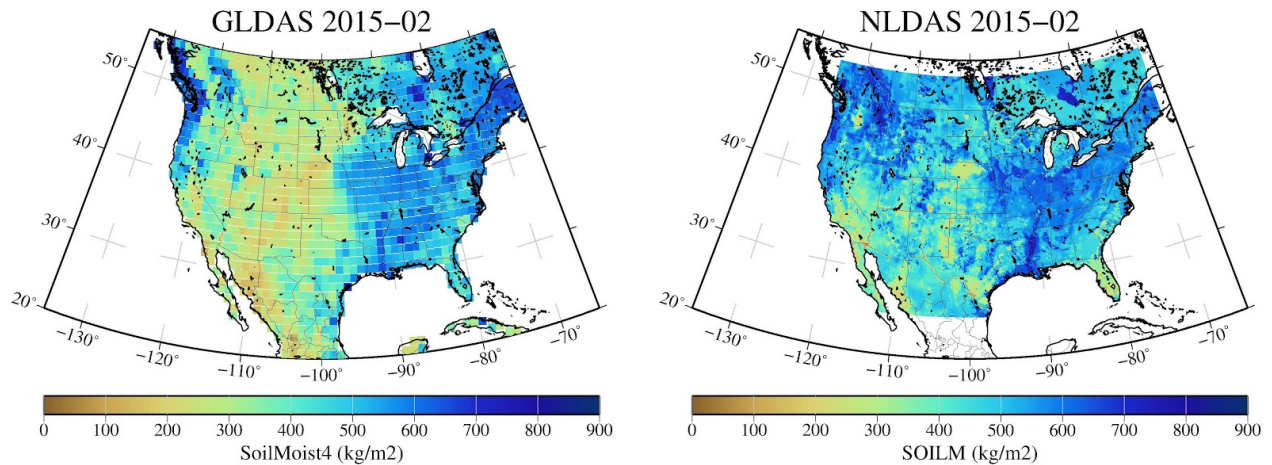


Figure 10. Comparison of soil moisture load in the GLDAS and NLDAS Noah models for February 2015. The color bars both refer to soil moisture but reflect the different variable names used in the data files.

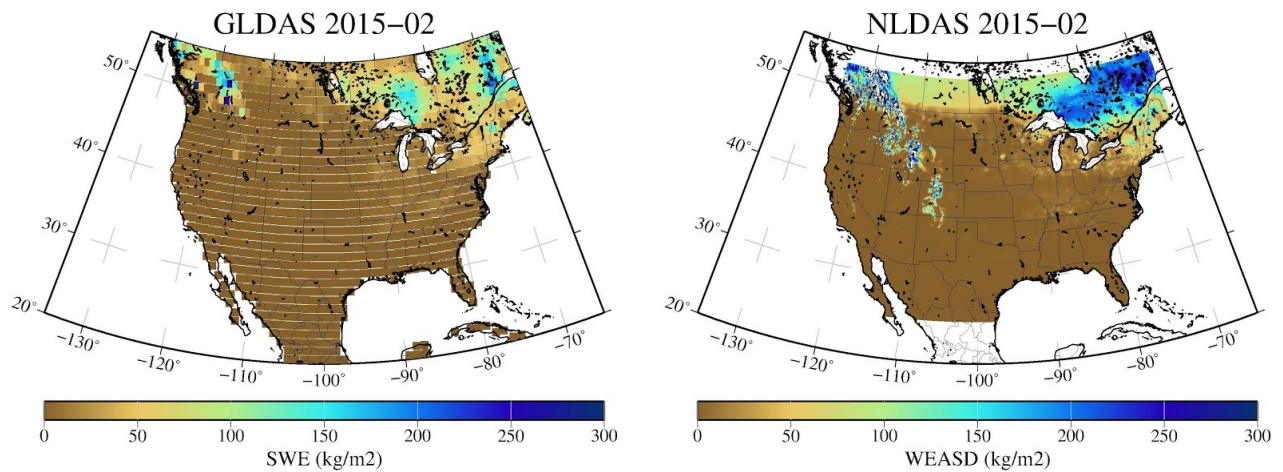


Figure 11. Comparison of snow load for the GLDAS and NLDAS Noah models in February 2015. The color bars both refer to snow-water-equivalent but reflect different variable names used in the data files.

Summary

Hydrologic signals observed at continuous GPS stations can be the result of 1) groundwater changes caused by natural and anthropogenic sources such as pumping for agriculture and cities, 2) surface water loading from water in soils and snowpack, and 3) surface water loading from natural lakes and reservoirs. UNAVCO produces displacement models based solely upon hydrologic surface water loading from water stored in soil, snow, and vegetation. Surface water loading models are made available to the geodetic and hydrologic communities to be used in research and teaching. The models illustrate an important hydrologic process, recording changes in the availability of surface water at seasonal and decadal scales.

Please see Appendix for description of model product access methods. Model products are accessible through FTP and web services. Currently UNAVCO produces displacement time series based on GLDAS v1. Displacement time series for NLDAS and GLDAS v2 are coming in 2017 and will necessitate some changes to the file naming and storage. GLDAS v1 products will be deprecated at some time after NLDAS and GLDAS v2 become available.

Useful Links

<https://disc.gsfc.nasa.gov> (Goddard Earth Sciences Data and Information Services Center Home Page)

<https://disc.gsfc.nasa.gov/hydrology/data-holdings/parameters> (index for definitions of environmental parameters in Land Surface Models)

<https://disc.sci.gsfc.nasa.gov/hydrology/documentation> (links to documentation, including README files for NLDAS and GLDAS and references)

<http://ldas.gsfc.nasa.gov/faq/> (NASA's Land Data Assimilation System FAQ)

<https://maps.waterdata.usgs.gov/mapper/> (USGS National Water Information System, map interface)

<http://data.cuahsi.org> (CUAHSI - Consortium of Universities for the Advancement of Hydrologic Science, Inc.)

Acknowledgements

Jeff McWhirter and Andy Wahr contributed substantially to the codes for this service. Additional feedback and assistance was provided by John Wahr, Stu Weir, Tonie Van Dam, and Adrian Borsa.

These hydrologic displacement models were generated at UNAVCO with funding through the GAGE Facility with support from the National Science Foundation (NSF) and National Aeronautics and Space Administration (NASA) under NSF Cooperative Agreement No. EAR-1261833.

The hydrologic environmental files used as the basis of our load model were based on data from NASA's Earth Science Division, archived and distributed by the Goddard Earth Sciences (GES) Data and Information Services Center (DISC).

References

Argus, D. F., Y. Fu, and F. W. Landerer, 2014, Seasonal variation in total water storage in California inferred from GPS observations of vertical land motion, *Geophys. Res. Lett.*, 41, doi:10.1002/2014GL059570.

Chen, F., K. Mitchell, J. Schaake, H.-L. Xue, V. Koren, Q.Y. Duan, M. Ek, and A. Betts, 1996, Modeling of land-surface evaporation by four schemes and comparison with FIFE observations, *J. Geophys. Res.*, 101 (D3), 7251–7268.

Ek, M. B., K. E. Mitchell, Y. Lin, E. Rogers, P. Grunmann, V. Koren, G. Gayno, and J. D. Tarpley, 2003, Implementation of Noah land surface model advances in the National Centers for Environmental Prediction operational mesoscale Eta model, *J. Geophys. Res.*, 108(D22), 8851, doi:10.1029/2002JD003296.

Fang, H., H. K. Beaudoin, M. Rodell, W. L. Teng, B. E. Vollmer, 2009, Global Land Data Assimilation System (GLDAS) products, services and application from NASA Hydrology Data and Information Services Center (HDISC), ASPRS 2009 Annual Conference, Baltimore, MD, 8-13 March 2009.

Koren, V., J. Schaake, K. Mitchell, Q. Y. Duan, F. Chen, and J. M. Baker, 1999, A parameterization of snow-pack and frozen ground intended for NCEP weather and climate models, *J. Geophys. Res.*, 104, 19 569–19 585.

Koster, R. D., and M. J. Suarez, 1992, Modeling the land surface boundary in climate models as a composite of independent vegetation stands, *J. Geophys. Res.*, 97(D3), 2697–2715, doi:10.1029/91JD01696.

Koster, R. D., and M. J. Suarez, 1996, Energy and water balance calculations in the Mosaic LSM, NASA Tech. Memo. 104606, Vol. 9, 76 pp.

Liang, X., D. P. Lettenmaier, E. F. Wood, and S. J. Burges, 1994, A simple hydrologically based model of land surface water and energy fluxes for GSMs, *J. Geophys. Res.*, 99 (D7), 14415–14428.

Fang, H., H. K. Beaudoin, M. Rodell, W. L. Teng, B. E. Vollmer, 2009, Global Land Data Assimilation System (GLDAS) products, services and application from NASA Hydrology Data and Information Services Center (HDISC), ASPRS 2009 Annual Conference, Baltimore, MD, 8-13 March 2009.

Fovell, R. G., and M.-Y. C. Fovell, 1993, Climate Zones of the Conterminous United States Defined Using Cluster Analysis, *J. Climate*, 6 (11), 2103–2135, doi:
[http://dx.doi.org/10.1175/1520-0442\(1993\)006<2103:CZOTCU>2.0.CO;2](http://dx.doi.org/10.1175/1520-0442(1993)006<2103:CZOTCU>2.0.CO;2).

Galloway, D.L., D.R. Jones, and S. E. Ingebritsen, 1999, Land subsidence in the United States: U.S. Geological Survey Circular 1182, 177 p.
<http://pubs.usgs.gov/circ/circ1182/>

Herring, T. A., T. I. Melbourne, M. H. Murray, M. A. Floyd, W. M. Szeliga, R. W. King, D. A. Phillips, C. M. Puskas, M. Santillan, L. Wang, 2016, Plate Boundary Observatory and Related Networks: GPS Data Analysis Methods and Geodetic Products, *Rev. of Geophys.*, 54, doi:10.1002/2016RG000529.

Meertens, C.M., C.M. Puskas, C. Molnar, and D.A. Phillips, 2016, Analysis of drought-related hydrologic loading signals from Plate Boundary Observatory GPS stations in the Sierra Nevada Mountains (Invited), Abstract G41C-01 presented a 2016 Fall Meeting, AGU, San Francisco, CA, December 12-16, 2016.

Meertens, C., J. Wahr, T. Van Dam, T. Herring, 2011, Detection and modeling of low amplitude deformation in the EarthScope Plate Boundary Observatory (PBO), Abstract G43C-08 presented at 2011 Fall Meeting, AGU, San Francisco, Calif., 5-9 Dec.

Miller, J. A. (1994). Ground Water Atlas of the United States. *Hydrogeology Journal*, 2(4), 59-62.

Mitchell, K.E., D. Lohmann, P.R. Houser, E.F. Wood, J.C. Schaake, A. Robock, B.A. Cosgrove, J. Sheffield, Q. Duan, L. Luo, R.W. Higgins, R.T. Pinker, J.D. Tarpley, D.P. Lettenmaier, C.H.

Marshall, J.K. Entin, M. Pan, W. Shi, V. Koren, J. Meng, B.H. Ramsay, and A.A. Bailey, 2004, The multi-institution North American Land Data Assimilation System (NLDAS): Utilizing multiple GCIP products and partners in a continental distributed hydrological modeling system, *J. Geophys. Res.*, 109, D07S90, doi:10.1029/2003JD003823.

Poland, J.F., Lofgren, B.E., Ireland, R.L., and Pugh, R.G., 1975, Land subsidence in the San Joaquin Valley, California as of 1972: U.S. Geological Survey Professional Paper 437-H, 78 p.
Rodell, M., P. R. Houser, U. Jambor, J. Gottschalck, K. Mitchell, C.-J. Meng, K. Arsenault, B. Cosgrove, J. Radakovich, M. Bosilovich, J. K. Entin, J. P. Walker, D. Lohmann, and D. Toll, 2004, The Global Land Data Assimilation System, *Bull. Amer. Meteor. Soc.*, 85(3): 381-394.

Rodell, M. and J. S. Famiglietti, 2002, The potential for satellite-based monitoring of groundwater storage changes using GRACE: the High Plains aquifer, Central US, *J. Hydrology*, 263(1), pp.245-256.

Rodell, M., J. Chen, H. Kato, J. S. Famiglietti, J. Nigro, C. R. and Wilson, 2007, Estimating groundwater storage changes in the Mississippi River basin (USA) using GRACE, *Hydrogeology Journal*, 15(1), pp.159-166.

Rui, H., and H. Beaudoin, 2016, README Document for Global Land Data Assimilation System Version 2 (GLDAS-2) Products, GES DISC.

Rui, H., 2011, README Document for Global Land Data Assimilation System Version 1 (GLDAS-1) Products, GES DISC.

Sheffield, J., G. Goteti, and E. F. Wood, 2006, Development of a 50-yr high-resolution global dataset of meteorological forcings for land surface modeling, *J. Climate*, 19 (13), 3088-3111.

van Dam, T., J. Wahr, P. C. D. Milly, A. B. Shmakin, G. Blewitt, D. Lavallee, and K. M. Larson, 2001, Crustal displacements due to continental water loading, *Geophys. Res. Lett.*, 28(4), 651-654, doi:10.1029/2000GL012120.

Wahr, J., M. Molenaar, and F. Bryan, 1998. Time variability of the Earth's gravity field: Hydrological and oceanic effects and their possible detection using GRACE. *J. Geophys. Res.*, 103(B12), pp.30205-30229.

Wahr, J., S. A. Khan, T. van Dam, L. Liu, J. H. van Angelen, M. R. van den Broeke, and C. M. Meertens, 2013, The use of GPS horizontals for loading studies, with applications to northern California and southeast Greenland, *J. Geophys. Res. Solid Earth*, 118, 1795–1806, doi:10.1002/jgrb.50104.

Xia, Y., K. Mitchell, M. Ek, J. Sheffield, B. Cosgrove, E. Wood, L. Luo, C. Alonge, H. Wei, J. Meng, B. Livneh, D. Lettenmaier, V. Koren, Q. Duan, K. Mo, Y. Fan, and D. Mocko, 2012,

Continental-scale water and energy flux analysis and validation for the North American Land Data Assimilation System project phase 2 (NLDAS-2): 1. Intercomparison and application of model products, *J. Geophys. Res.*, 117, D03109, doi:10.1029/2011JD016048.

Appendix. How to access UNAVCO Hydrologic Model Load Displacements

UNAVCO produces model displacements from surface loading for GLDAS for different land surface models (NOAH, Mosaic, VIC) with 1° grids

FTP Access

Time series files produced by the model are available at the UNAVCO ftp site <ftp://data-out.unavco.org/pub/products/hydro>

Index of <ftp://data-out.unavco.org/pub/products/hydro/>

 [Up to higher level directory](#)

Name	Size	Last Modified
 mos10		6/20/14 12:00:00 AM
 noah025		6/20/14 12:00:00 AM
 noah10		6/20/14 12:00:00 AM
 vic10		6/20/14 12:00:00 AM

*note that noah025 has been discontinued.

The files are named with 4-char ID, model name, and .hyd extension. For example: AB13_NOAH10.hyd is for station AB13 and the NOAH 1 degree model.

Coming in 2017, subdirectories for NLDAS and GLDAS v2 will be added to the ~/hydro directory. The new files will be available from <ftp://data-out.unavco.org/pub/products/hydro/NLDAS2> and <ftp://data-out.unavco.org/pub/products/hydro/GLDAS2>. Data files within these subdirectories will have the format $\{\text{4-charID}\}_{\{\text{LSM_MODEL}\}}_{\{\text{DAS_MODEL}\}}.hyd$. For example, AB13_NOAH10_GLDAS2.hyd

Web Services Access

Hydrologic files can be downloaded from UNAVCO's new web services (preferred access method) at <http://www.unavco.org/data/web-services/documentation/documentation.html#!/hydro/getHydrologicalByStationId>.

These data products are available for all GAGE-processed GPS stations inside the LSM grids. Three sets of LSMs are used to produce three sets of surface water loading models at the coordinates of each GPS station.

To see a tutorial video on UNAVCO's web services please see:

<http://www.unavco.org/data/web-services/web-services.html>

The web services are organized and documented using the Swagger specification for RESTful web services. Go to the "hydro" entry and click on the link (Figure A1). The response is shown in the screen capture below (Figure A2). Enter the 4-character station ID, starttime, endtime, and hydro model (noah10, mos10, vic10), and output at text/csv or plain text (no commas) then click on "Try it out!".

Note that this is currently a beta version. After a commissioning period this will be moved out of beta and assigned a version number.

GET /hydro/model/load/displacement/{station}/beta Hydrological Loading Webservice

Implementation Notes
Outputs Hydrological Loading Timeseries. Hydrological products are displacement models calculated at GPS/GNSS station coordinates and based on loading from water stored as snowpack, soil moisture, and in vegetation.

Response Class (Status 200)
string

Response Content Type:

Parameters

Parameter	Value	Description	Parameter Type	Data Type
station	<input type="text" value="P201"/>	The four character station identifier. Example: P201.	path	string
starttime	<input type="text" value="2008-01-01"/>	Select the starting datetime of the time series search range (ISO 8601).	query	string
endtime	<input type="text" value="2008-03-01"/>	Select the ending datetime of the time series search range (ISO 8601).	query	string
model	<input type="text" value="noah10 (default)"/>	Select the land surface model for calculating hydrological loading.	query	string

Response Messages

HTTP Status Code	Reason	Response Model	Headers
400	Invalid query parameters.		
404	Invalid Station id supplied, or no data for specified query.		
500	Uncaught internal error.		
502	Error connecting to external server.		
503	Internal error.		

[Hide Response](#)

Figure A1. Swagger page for the default example site P201. The user can choose station 4-char ID, starttime, endtime, and model.

Curl

```
curl -X GET --header 'Accept: text/csv' 'http://web-services-beta.int.unavco.org/hydro/model/load/displacement/P201/beta?starttime=2008-01-01&endtime=2008-03-01&model=noah10'
```

Request URL

```
http://web-services-beta.int.unavco.org/hydro/model/load/displacement/P201/beta?starttime=2008-01-01&endtime=2008-03-01&model=noah10
```

Response Body

```
# dataset: GeoCSV 2.0
# field_unit: ISO 8601 date UTC, meters, meters, meters
# field type: string, float, float, float
# attribution: http://www.unavco.org/community/policies_forms/attribution/attribution.html
# Request URI: http://web-services-beta.int.unavco.org/hydro/model/load/displacement/P201/beta?starttime=2008-01-01&endtime=2008-03-01&model=noah10
# Approximate Station Coordinate: Latitude: 38.559800 Longitude: -122.658400
# Source File: ftp://data-out.unavco.org/pub/products/hydro/noah10/p/P201_NOAH10.hyd Date: 2017-01-20 20:14:02
# Land Surface Model: noah10
# Land Surface Model grid size (degrees): 1.0
Date, DispN, DispE, DispU
2008-01-01, 0.00032, 0.00019, -0.00097
2008-01-02, 0.00034, 0.00020, -0.00105
2008-01-03, 0.00035, 0.00022, -0.00113
2008-01-04, 0.00037, 0.00024, -0.00121
2008-01-05, 0.00039, 0.00025, -0.00129
2008-01-06, 0.00040, 0.00027, -0.00137
2008-01-07, 0.00042, 0.00028, -0.00145
2008-01-08, 0.00044, 0.00030, -0.00153
2008-01-09, 0.00045, 0.00032, -0.00161
2008-01-10, 0.00047, 0.00033, -0.00169
2008-01-11, 0.00048, 0.00035, -0.00177
2008-01-12, 0.00050, 0.00036, -0.00185
2008-01-13, 0.00052, 0.00038, -0.00193
```

Response Code

```
200
```

Response Headers

```
{
  "content-type": "text/csv; charset=utf-8",
  "cache-control": "public, max-age=60",
  "expires": "Fri, 03 Feb 2017 18:36:04 GMT"
}
```

Figure A2. Example response body for a web services query. The first box (Curl) in the response is a sample curl script that can be used to help automate the web service response. The curl command can be built into a shell script that directs the output to a local file. The second box (Request URL) is the simple RESTful URL that can be used in a browser. The Response Body shows the output in GeoWS CSV format that was developed with IRIS and others from EarthCube. The model output is given in Date, DispN (north displacement), DispE (east displacement), and DispU (vertical displacement).